Remote sensing of the magnetospheric plasma density using ground-based magnetometer networks

M. Vellante[1], A. Del Corpo[1], E. Pietropaolo[1],

M. Piersanti[1], B. Heilig[2]

1. *Department of Physical and Chemical Sciences, University of L'Aquila, Italy*
2. *Geological and Geophysical Institute of Hungary, Tihany, Hungary*

101° Congresso della
Società Italiana di Fisica
Roma, 21 - 25 Settembre 2015

Geomagnetic Field Line Resonances (FLR)

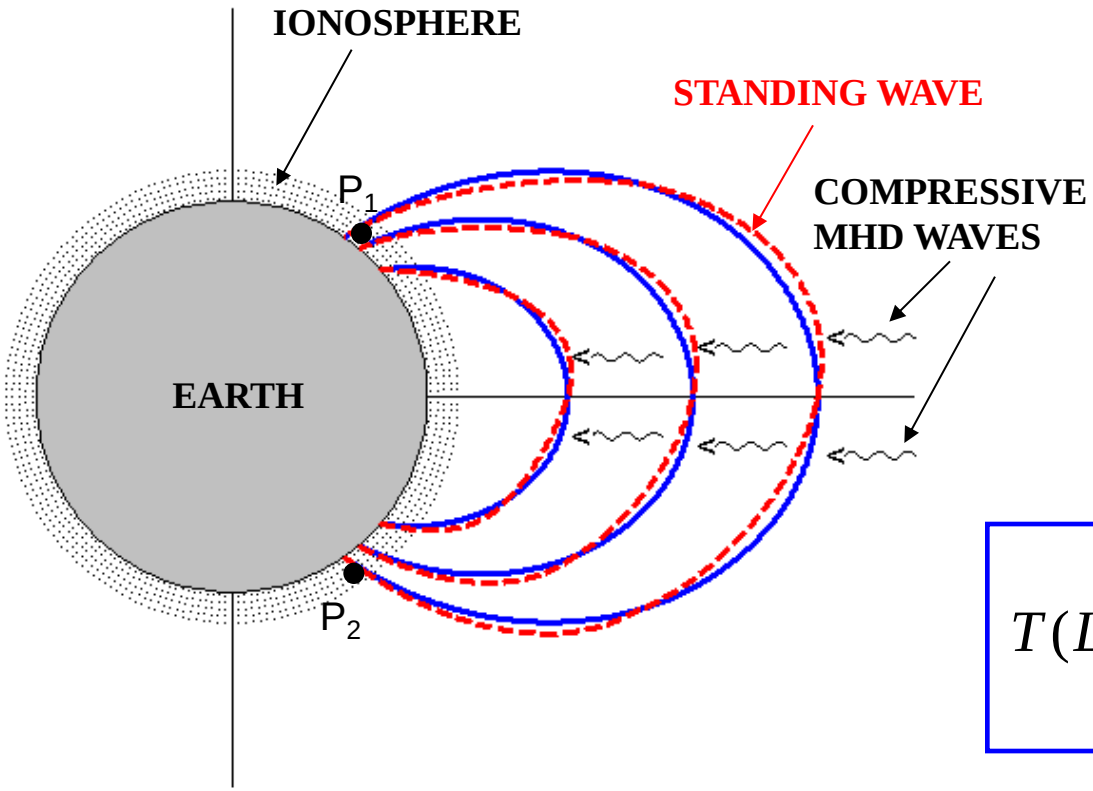

Fundamental eigenperiod

$$T(L) \cong 2\int_{P_1}^{P_2} \frac{ds}{V_A(s)}$$

$\mathbf{V_A}$: Alfvén velocity

$$T(L) = 2\mu_o^{1/2} \int_{P_1}^{P_2} \frac{\rho^{1/2}(s)}{B(s)}\, ds$$

In the plasmasphere (L< 4):

10 s < T < 100 s

FLR: a useful tool for

- **Validating models of the plasma distribution in the magnetosphere**
- **Monitoring temporal variations of the plasma density**

Inference of the plasma mass density from field line eigenfrequencies

Standard procedure for low and middle latitudes:

Assumption: Observed FLR frequencies (f_R) correspond to the axisymmetric **toroidal** mode eigenfrequencies in a **dipole** field.

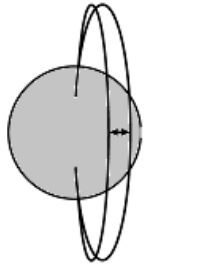
Toroidal Mode

Governing equation:

$$d^2E/dz^2 + \lambda\,(1- z^2)^6\,\rho(z)/\rho_o\,E = 0$$

E : wave electric field
z = cos (θ), **θ**: colatitude
ρ : mass density along the field line
ρ_o: equatorial mass density

Eigenvalues **λ** are found imposing:

1) the boundary condition: **E = 0** at the altitude (100-200 km) where the wave is reflected

2) A given functional form for the mass density along the field line.

Common assumption: $\rho(r)/\rho_o = (r/r_o)^{-m}$

For any given **L- shell** and **m** value, the inferred **equatorial** mass density is:

$$\tilde{\rho}_o = \frac{B_E^2}{4\pi^2 \mu_o R_E^2}\,\frac{\lambda(L,m)}{L^8 f_R^{\,2}}$$

For a given L ⇒ $\tilde{\rho}_o = \dfrac{\text{const}\,(L,m)}{f_R^{\,2}}$

Effects of external sources

At high latitudes, and even at low and middle latitudes during disturbed conditions (*Berube et al*., 2006), need to consider geomagnetic field geometry more realistic than dipole or IGRF geometry (i.e. *Tsyganenko* models).

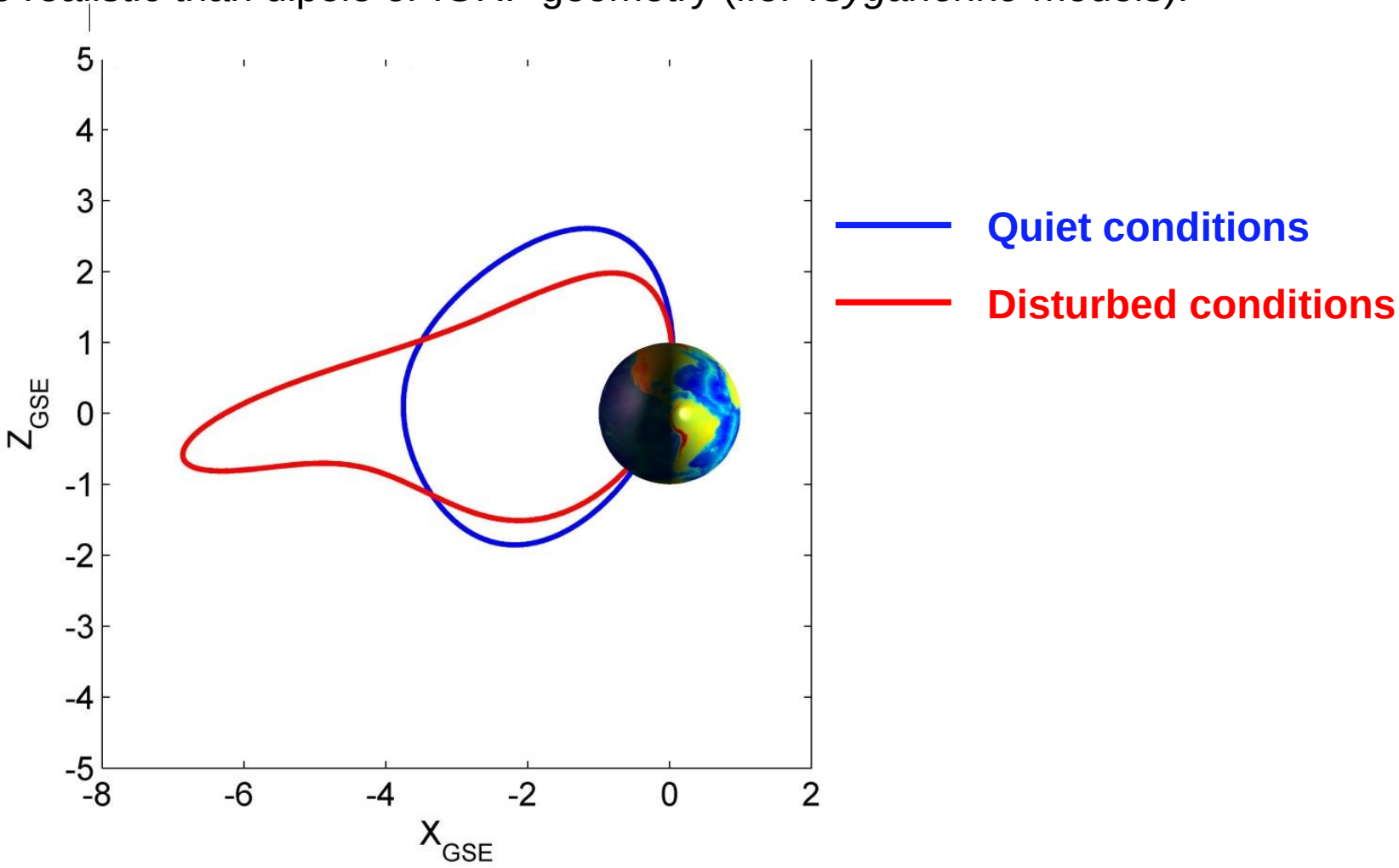

GRADIENT METHOD FOR DETECTING FIELD LINE RESONANCES FROM GROUND-BASED ULF MEASUREMENTS

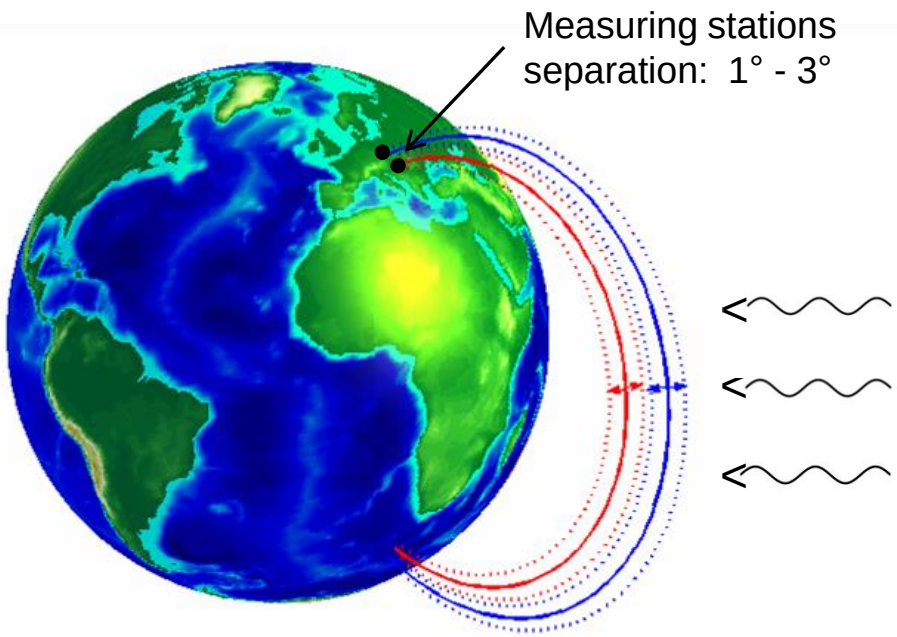

— **Higher latitude field line**
Lower resonance frequency (f_N)

— **Lower latitude field line**
Higher resonance frequency (f_S)

FREQUENCY RESPONSE OF TWO OSCILLATORS

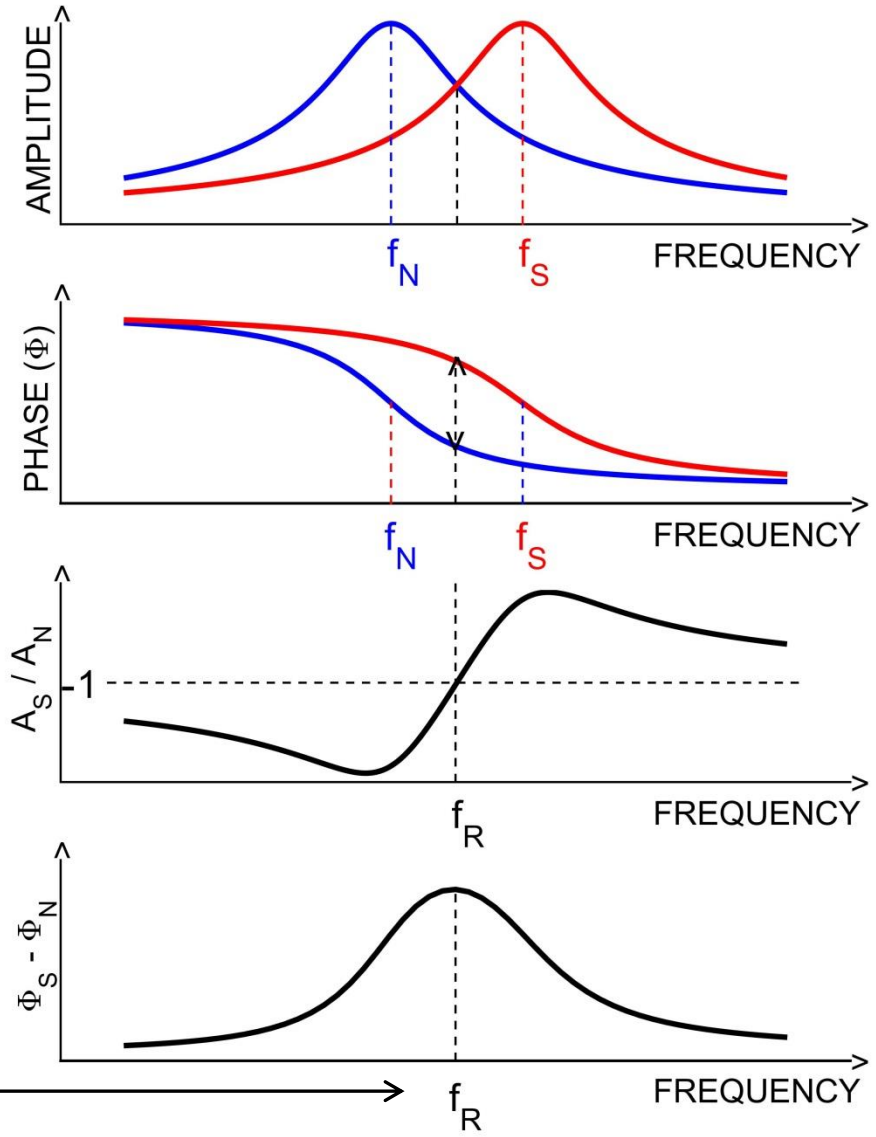

CROSS-PHASE TECHNIQUE

Resonance frequency at the middle point.

Identified by a maximum in the phase difference

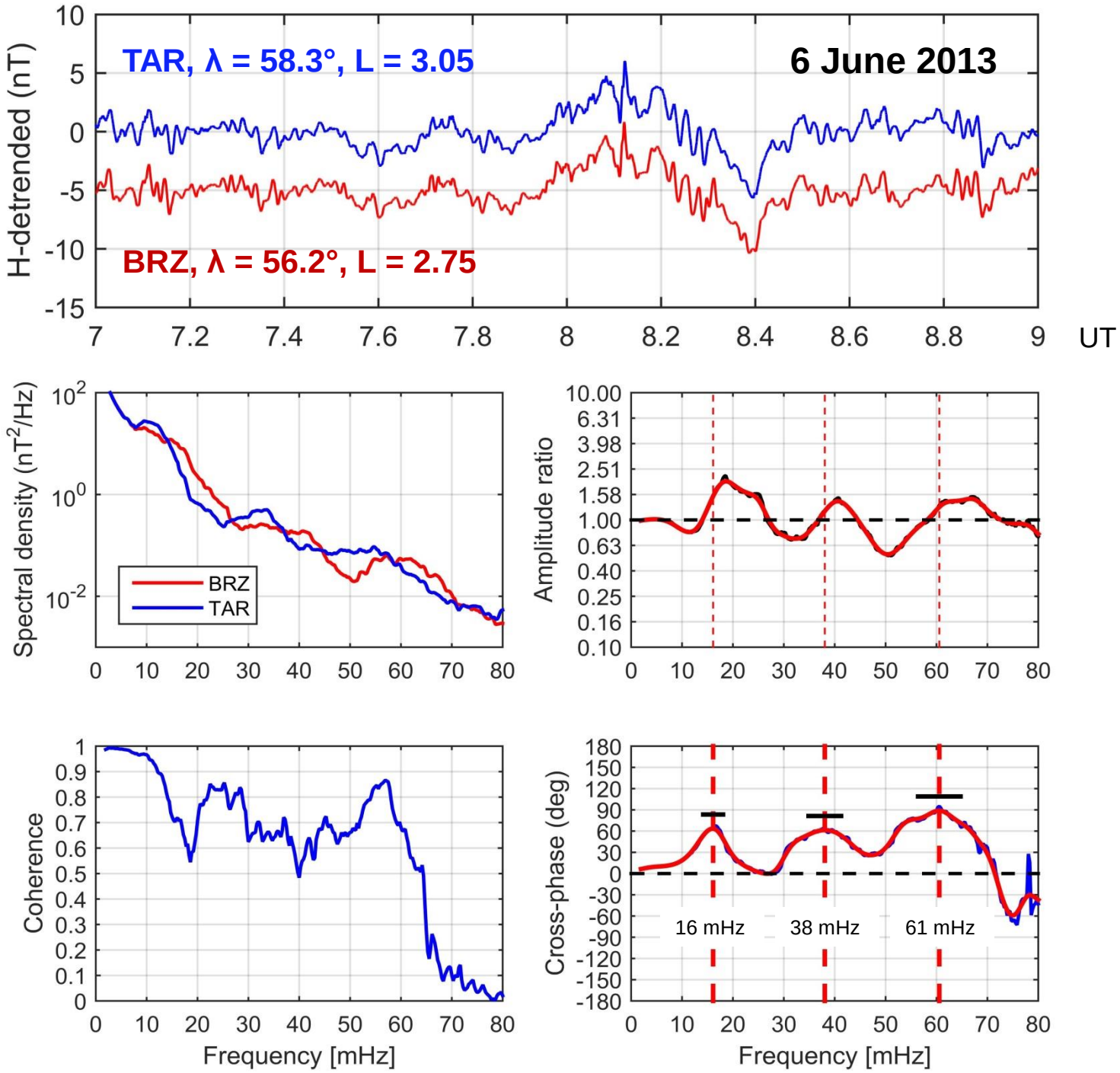
TAR, λ = 58.3°, L = 3.05
6 June 2013
BRZ, λ = 56.2°, L = 2.75
H-detrended (nT)
UT
Spectral density (nT²/Hz)
BRZ
TAR
Amplitude ratio
Coherence
Frequency [mHz]
Cross-phase (deg)
16 mHz
38 mHz
61 mHz
Frequency [mHz]

CROSS-SPETTRI DINAMICI

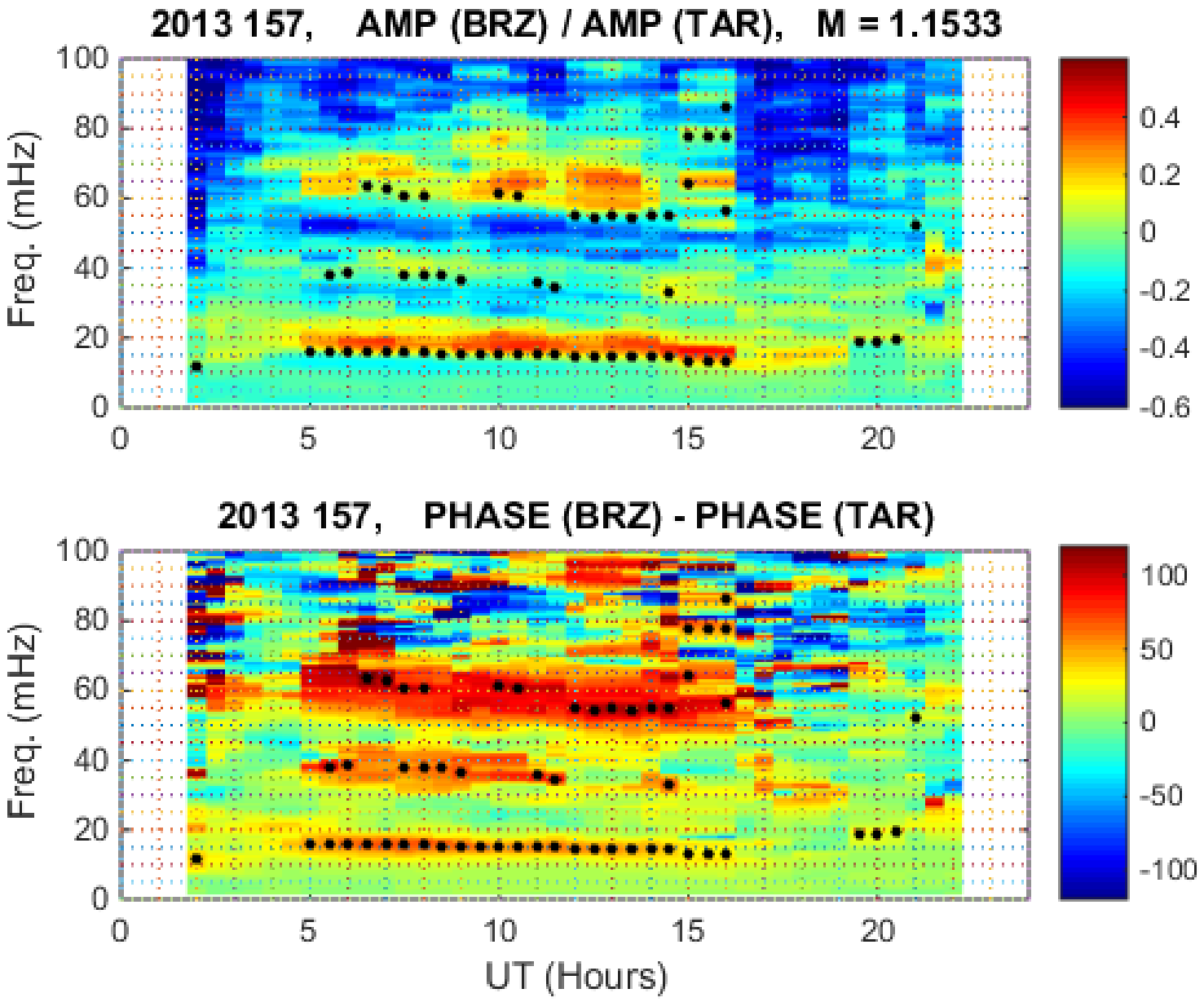

SEGMA (South European GeoMagnetic Array)
(1.56 < L < 1.88)

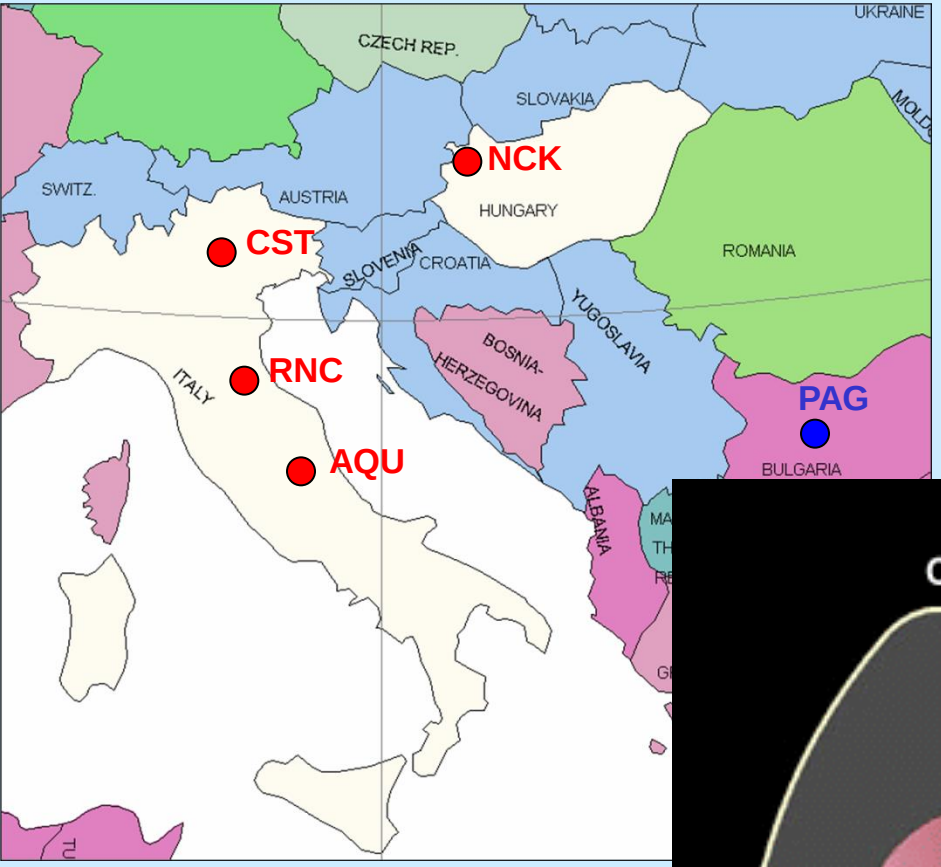

3 gradient installations

Stations	Latitud. separ.	L
NCK - CST	1.9°	1.83
CST - RNC	2.5°	1.71
RNC - AQU	1.9°	1.61

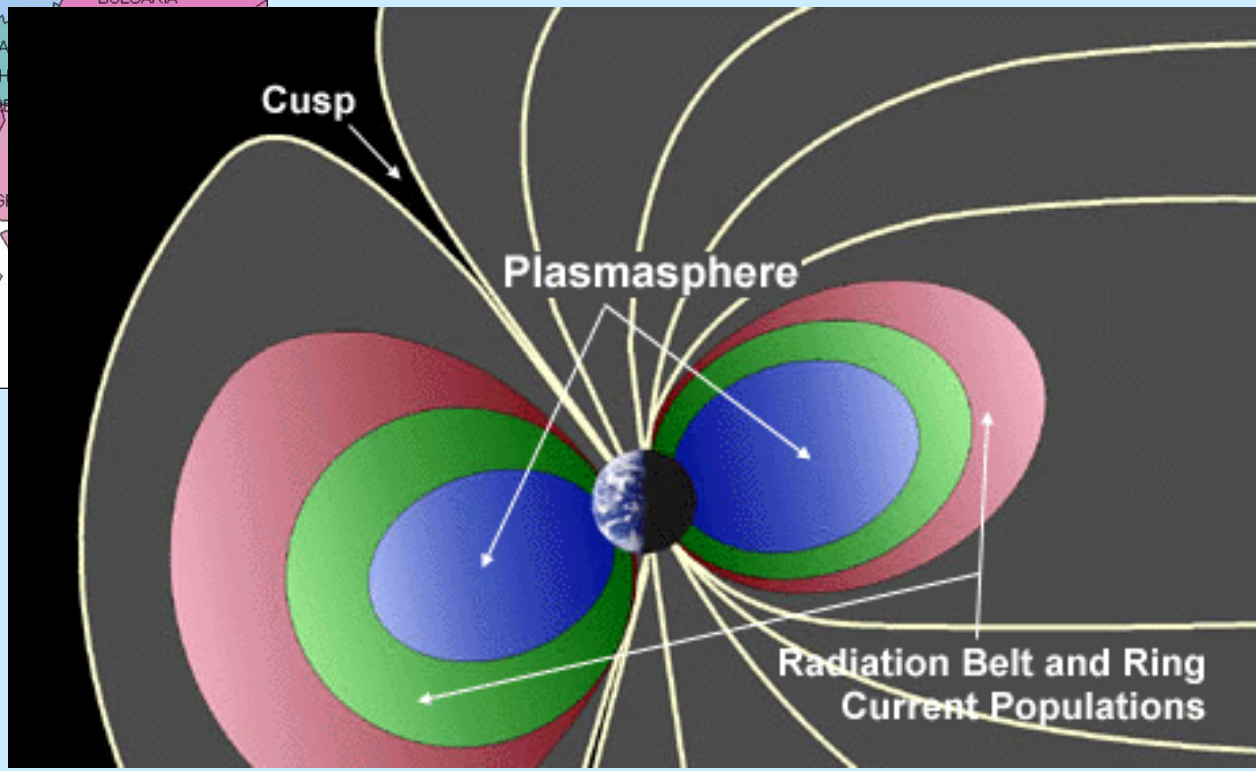

Cooperation between:

- **University of L'Aquila (Italy)**
- **Space Res. Inst. of Graz (Austria)**

Diurnal variation

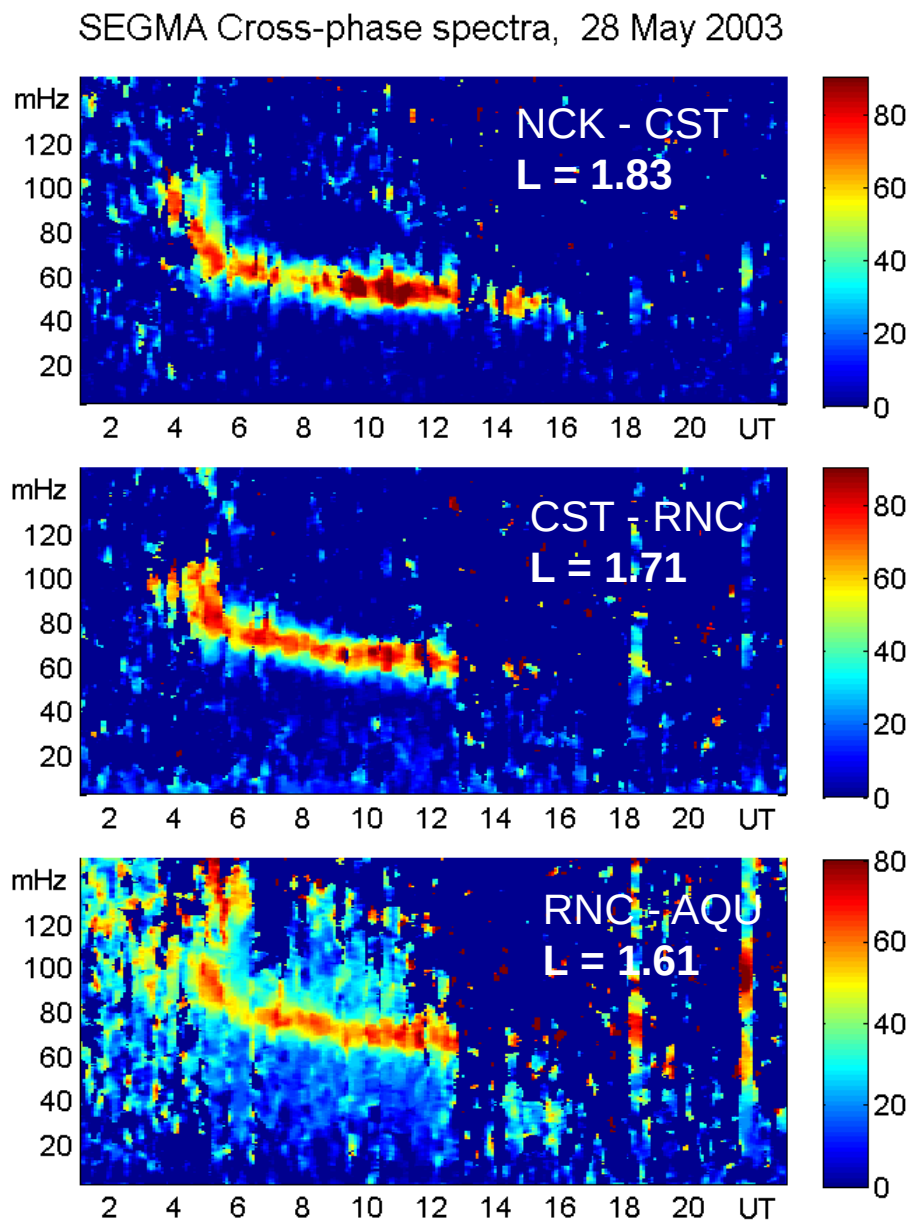

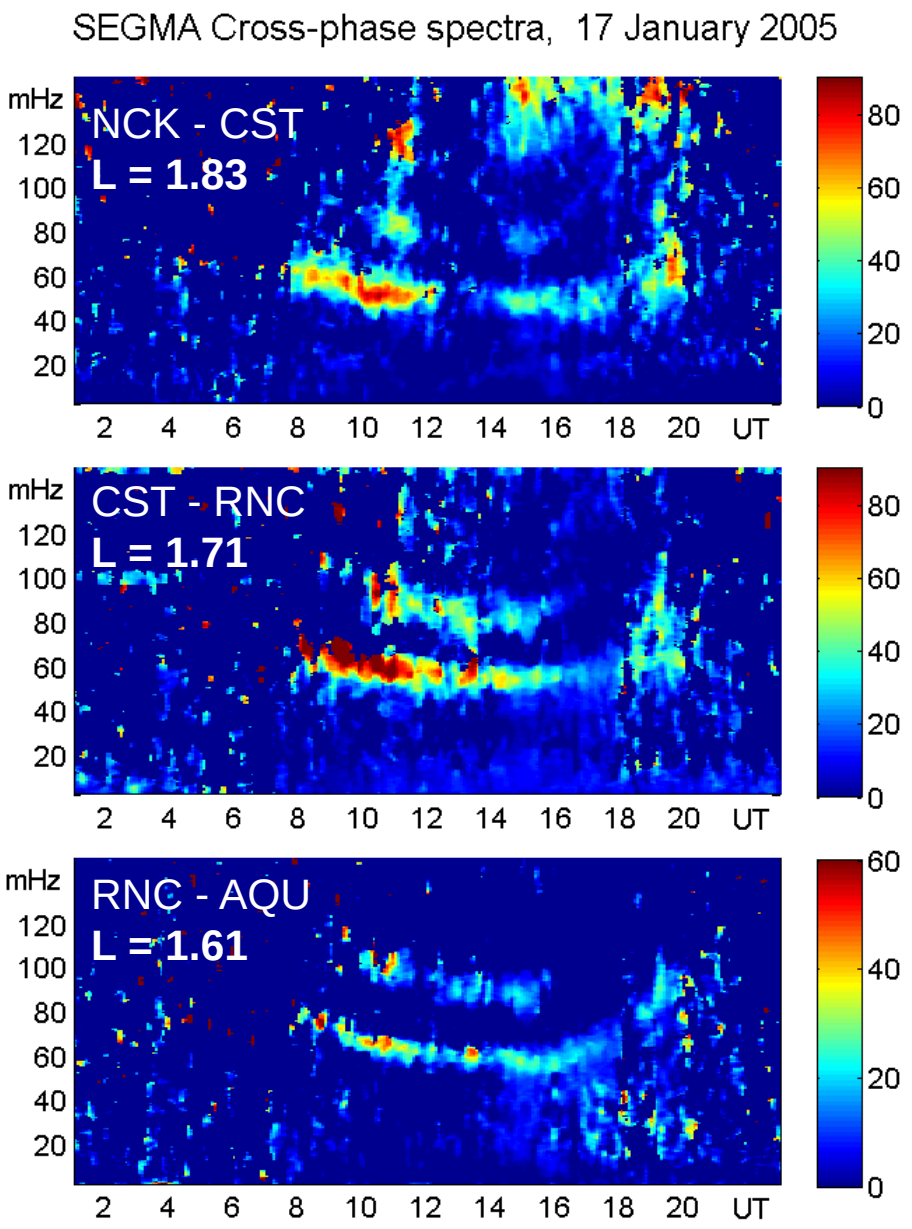

ANNUAL VARIATION OF THE FLR FREQUENCY AT L = 1.61, YEAR 2003

DAILY AVERAGES (0900 – 1600 LT)

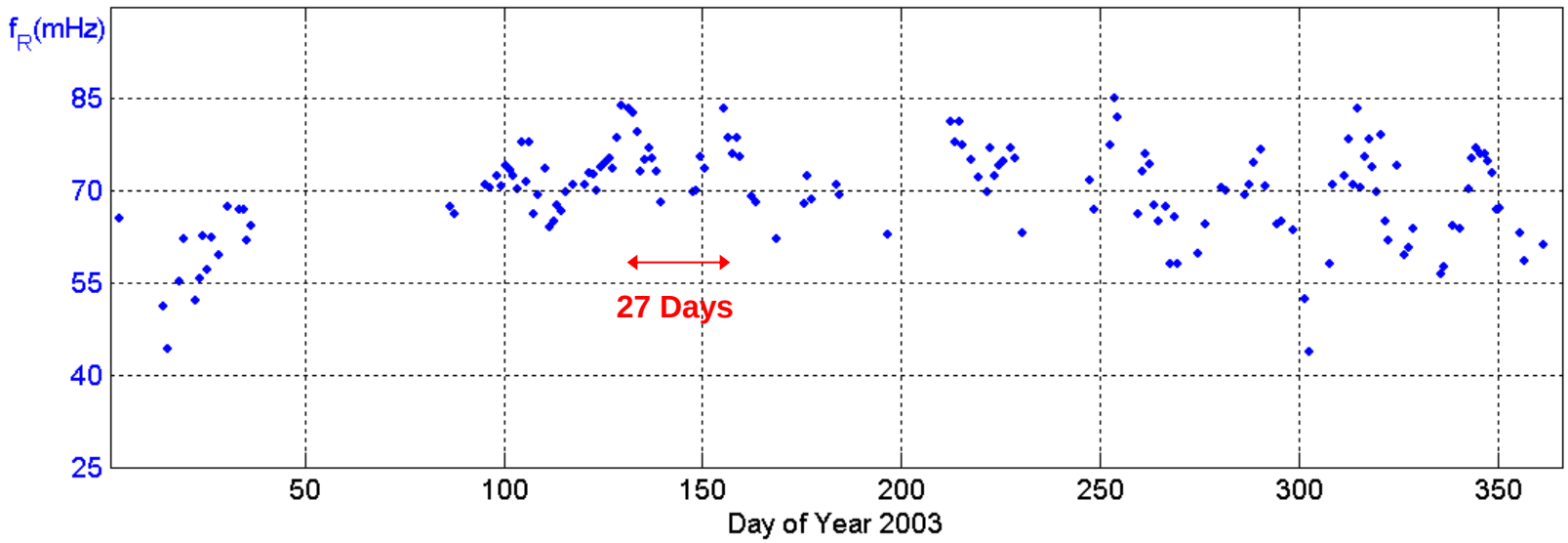

- **a nearly 27-days modulation appears which must be connected to the recurrence of active regions of the Sun**

SOLAR IRRADIANCE DEPENDENCE OF THE FLR FREQUENCY (L = 1.61)

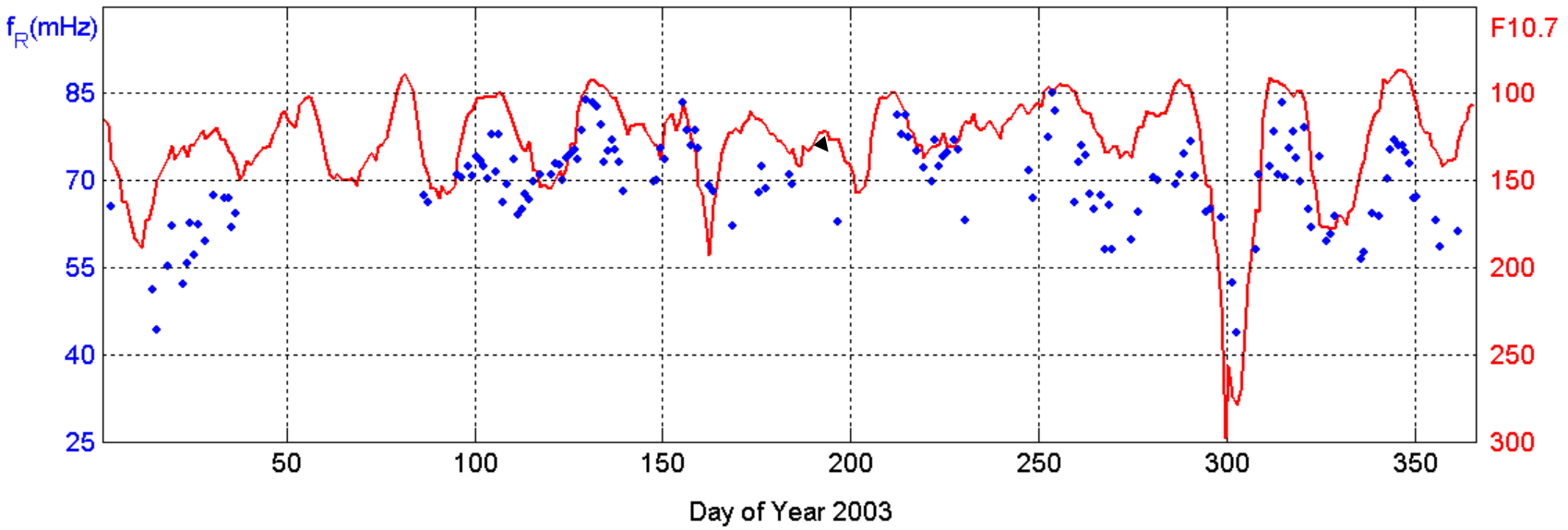

Combined effects of solar and geomagnetic activity

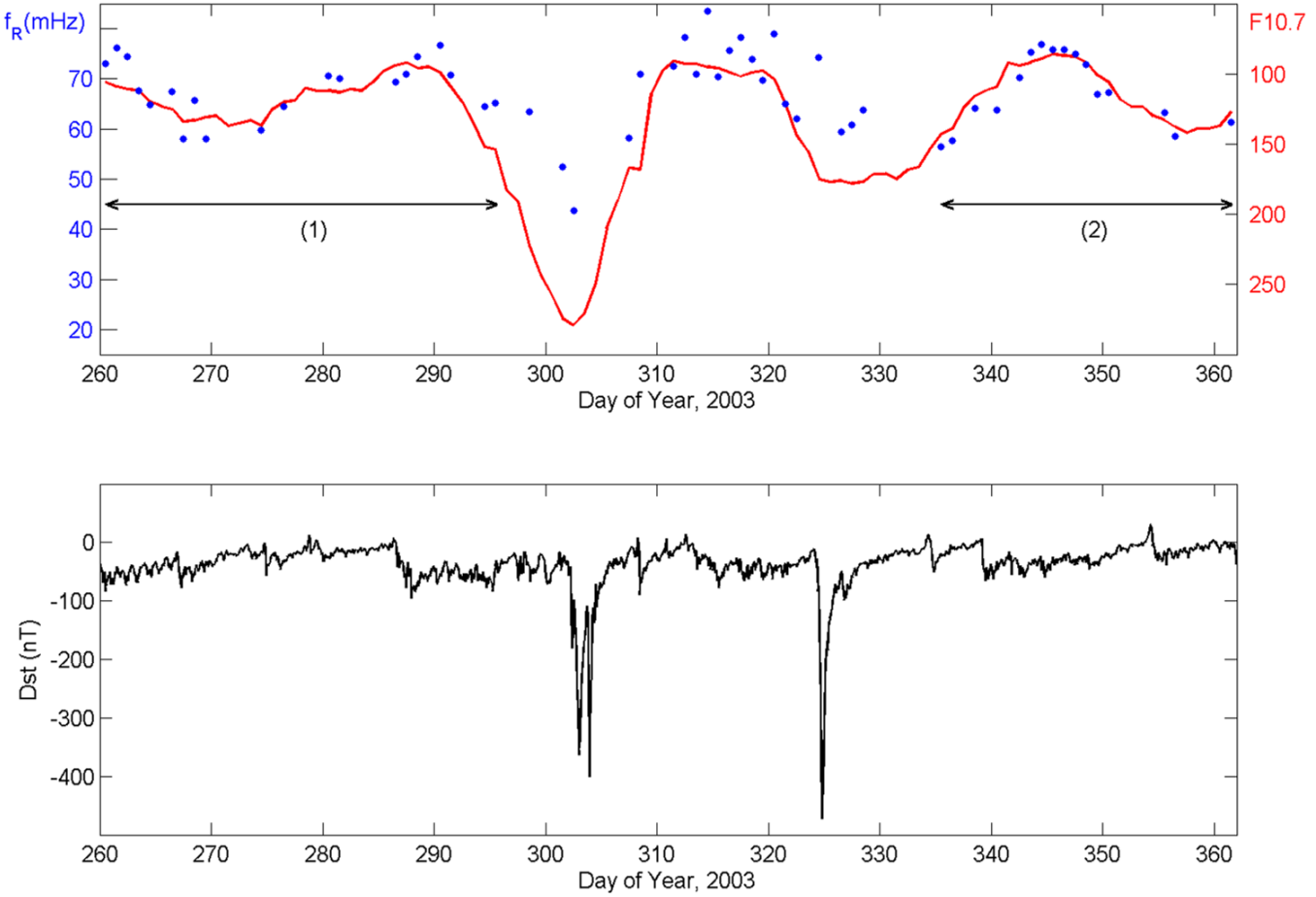

Under quiet magnetospheric conditions (intervals 1 and 2), the plasmaspheric density (as inferred by the FLR frequency: $\rho \sim f_R^{-2}$) is strongly controlled by the solar EUV radiation (F10.7 index).

During disturbed magnetospheric conditions (high **Dst** index) f_R is higher than what expected.

The inferred plasmaspheric density depletion is possibly due to plasmasphere erosion by the enhanced magnetospheric convection electric field and/or to enhanced ion loss rate in the ionosphere.

Mid-continent MAgnetoseismic Chain (McMAC):

A Meridional Magnetometer Chain for Magnetospheric Sounding

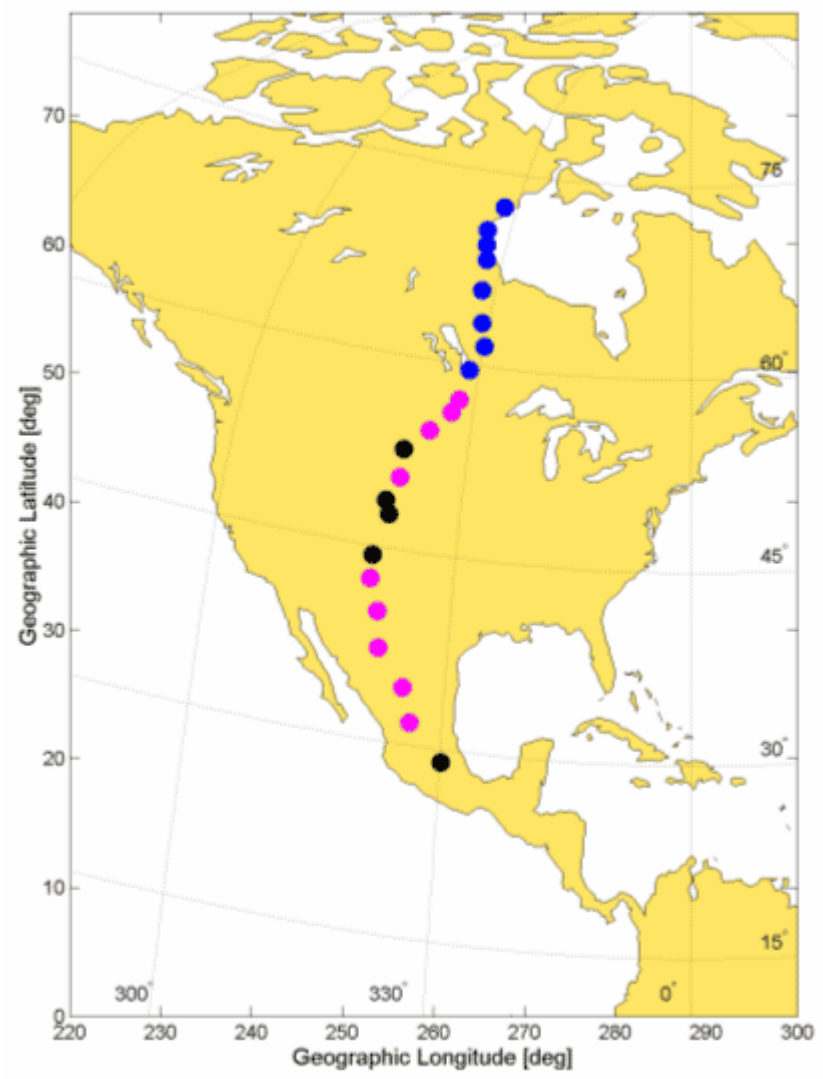

$1.3 < L < 11.7$

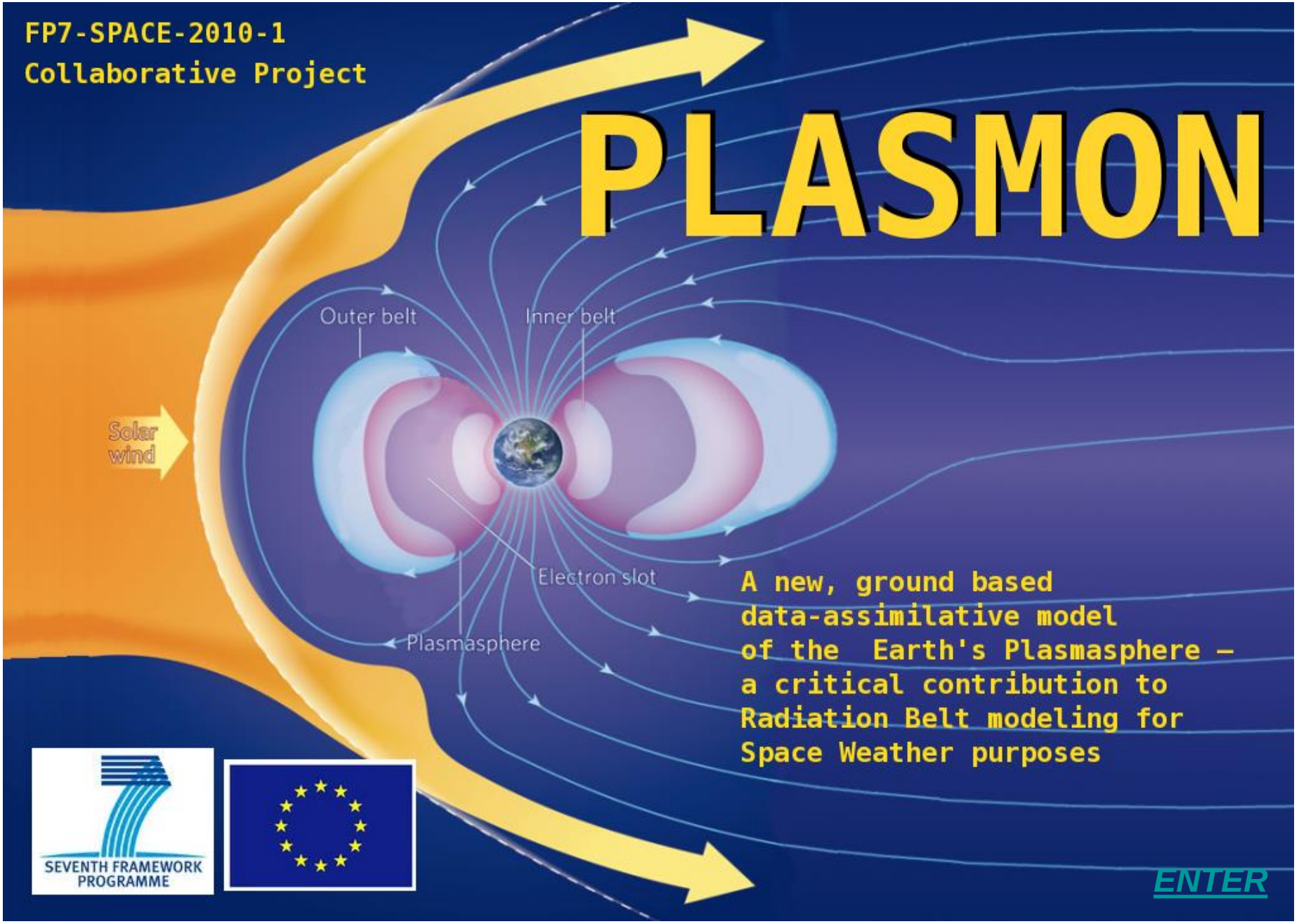

Tematica di riferimento: Security of space assets from space weather events

EMMA (1.5 < L < 6.5)

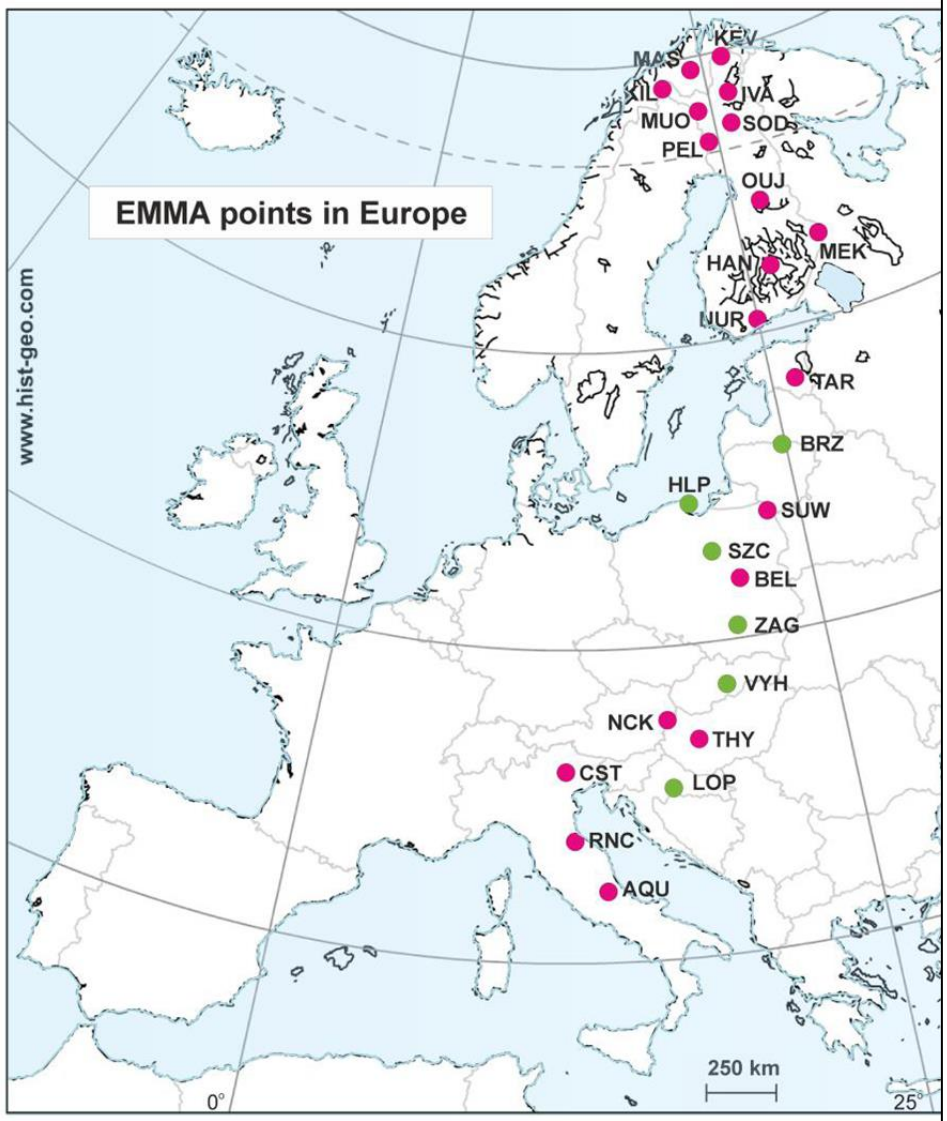

25 stations, all equipped with high sensitivity fluxgate magnetometers and GPS antenna for precise time recording.

All stations are remotely connected and transmit data to local servers every 1-15 min.

Data are collected at two main servers (one in Hungary and the other at University of L'Aquila) which continuously monitor the operational status of the whole network, and cyclically (every 15 min) run a procedure to detect FLR frequencies from several station pairs and deduce in near real time the equatorial plasma mass density in the *L*-range 1.6-6.1.

EMMA-Net Data Flow

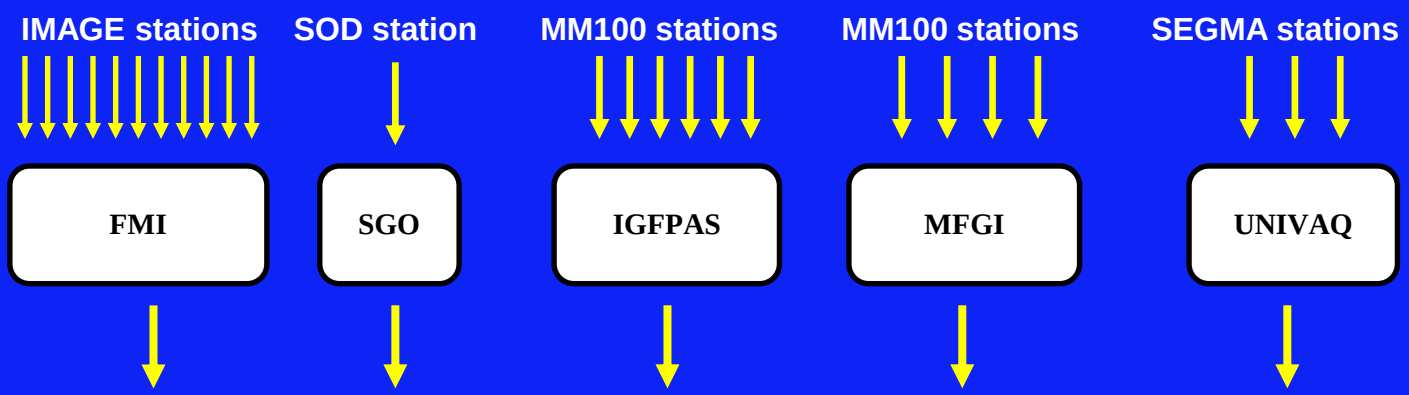

PLASMON EMMA Servers (L'Aquila; Tihany)

- **Conversion to EMMA Data Format (FMI stations)**
- **Transformation: XYZ → HDZ (if necessary)**
- **Removal of spikes, check of timing – correction**

Tihany Server

- **Implementation of FLRID**
- **Web-based monitor (http://geofizika.canet.hu/plasmon/):**

  near real time magnetograms/power spectra/FLRID results

L'Aquila Server

- **Implementation of FLRID**
- **Implementation of FLRINV:**

  results are stored in daily text files updated every 15 min and available for downloading

http://plasmonserver.aquila.infn.it/EMMA_FLR_DENSITY

EMMA for PLASMON and Tihany Geophysical Observatory Geomagnetic pulsation data

EMMA Home
Map
Coordinates
Instruments
MFGI home

Latest
Plot
PSD spectra
CSD spectra

Archive
Availability
PSD spectra
CSD spectra

Space Weather

Space Climate

Publications

IHY2007
IHY CIP39
WHI campaign

Contact

Staff

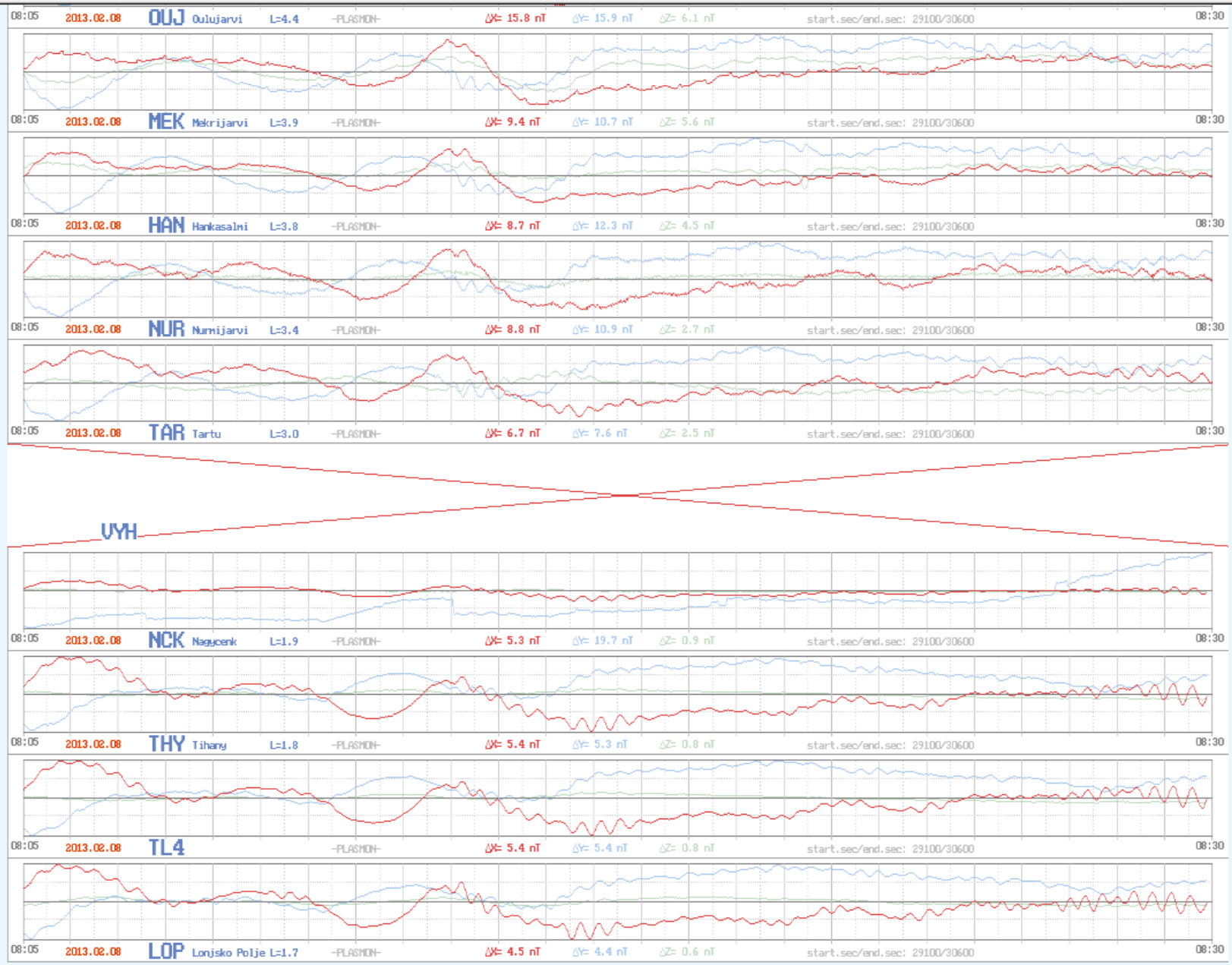

EMMA for PLASMON and Tihany Geophysical Observatory Geomagnetic pulsation data

EMMA Home
Map
Coordinates
Instruments
MFGI home

Latest
Plot
PSD spectra
CSD spectra

Archive
Availability
PSD spectra
CSD spectra

Space Weather

Space Climate

Publications

IHY2007
IHY CIP39
WHI campaign

Contact

Staff

EMMA Power Spectral Densities (latest 4 days)

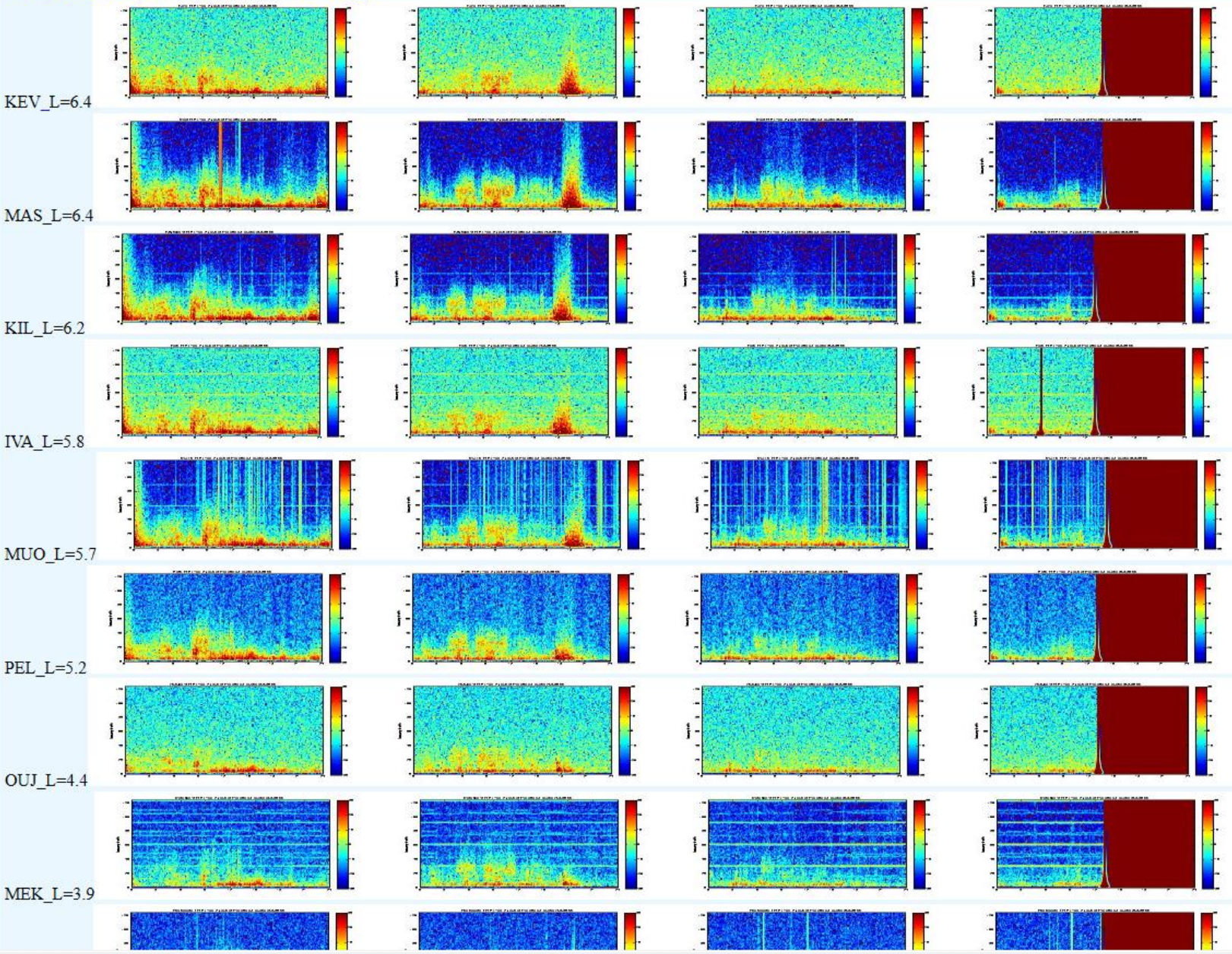

EMMA for PLASMON and Tihany Geophysical Observatory Geomagnetic pulsation data

OUJ-HAN L=4.09

HAN-NUR L=3.62

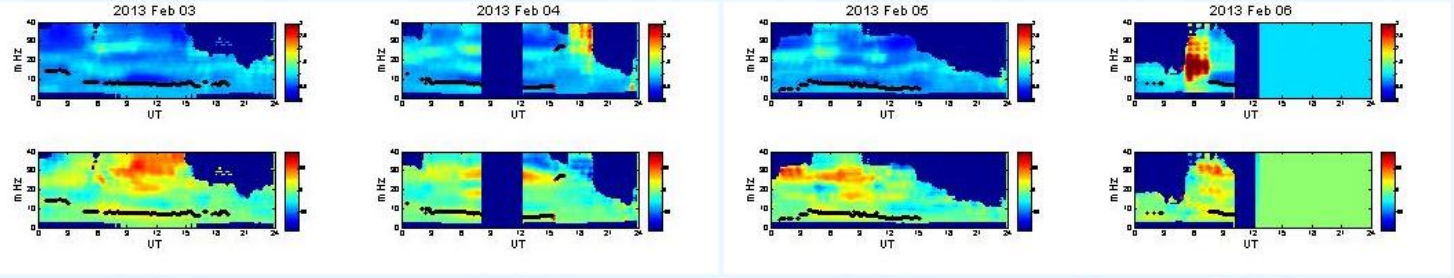

NUR-TAR L=3.24

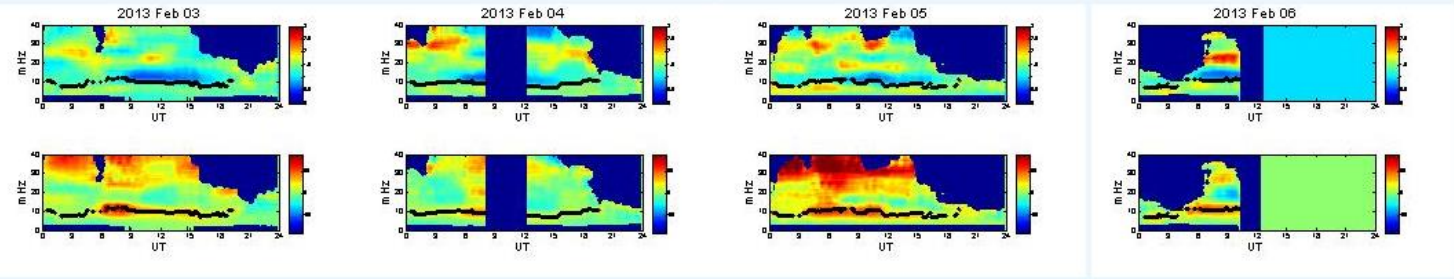

NCK-LOP L=1.81

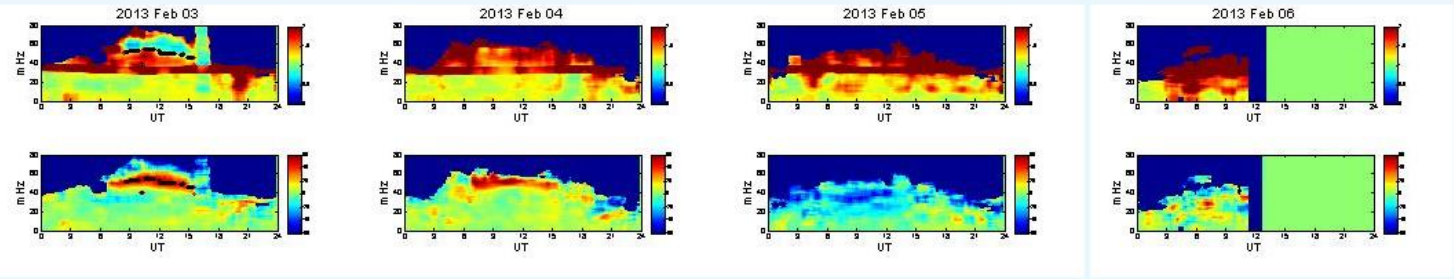

THY-LOP L=1.78

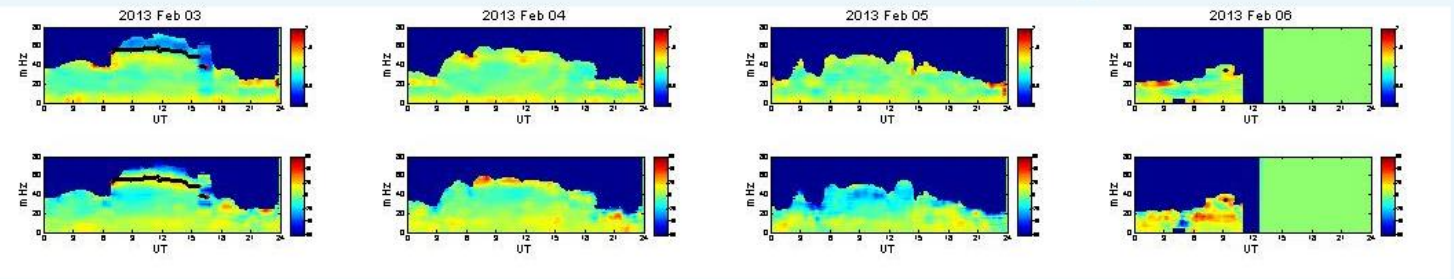

Under development

Last modified: 2012-03-09 11:20:39

FLR inversion (FLRINV)

The inversion algorithm converts FLR frequencies into estimates of the equatorial plasma mass density ρ_{eq} ($1.6 < L < 6.3$).

It solves numerically the MHD wave equation for the toroidale mode in an arbitrary field geometry (dipole, IGRF, **T01** models) and for a given density distribution along the field line: $\rho(s) = \rho_{eq} (r / r_{eq})^{-m}$, and infers ρ_{eq}.

T01 model (Tsyganenko, 2002). Input parameters:

- Universal Time: to determine the proper coefficients of the internal field (IGRF) and the tilt angle;
- Solar wind dynamic pressure;
- Dst index;
- IMF By and Bz components;
- G1, G2: take into account the prehistory state of the magnetosphere (determined by By, Bz, Vsw of the previous hour).

Near Real-time FLRINV process

Run every 15 min using:

- quasi real-time values of field line eigenfrequencies of all available station pairs (as computed by FLRID);
- solar wind and Dst parameters.

Real time solar wind data taken from the NOAA Space Weather Prediction Center which provides the latest 2 hours of magnetic and plasma data of the ACE satellite located at the L1 libration point: http://services.swpc.noaa.gov/text/ace-magnetometer.txt; http://services.swpc.noaa.gov/text/ace-swepam.txt

Data are time-shifted to take into account the propagation time of the solar wind from the satellite position to the Earth (typically about 1 hour).

Propagated data are resampled at fixed times and hourly running averages (time step 1 min) are produced.

Real-time Dst data are taken from the Dcx server of the University of Oulu, Finland:

http://dcx.oulu.fi/DstDcxDxtData/RealTime/Dxt/DxtRT.txt

Extract of an online output file

PAIR	L	YEAR	DOY	HOUR-UT	LT	**Req**	mHz	amu/cc	HOUR(SW)	BY	BZ	P	HOUR(G)	G1	G2	HOUR(DST)	DST
masmuo	6.012	2014	185	10.72	12.89	**6.207**	23.1	1.01e+00	10.72	-2.6	2.1	0.9	10.22	0.81	0.52	10.72	-2.9
kilpel	5.691	2014	185	10.95	13.02	**5.845**	14.8	3.97e+00	10.95	-2.2	2.2	1.0	10.45	0.36	0.01	10.95	-2.9
muopel	5.450	2014	185	10.80	12.91	**5.622**	15.0	5.28e+00	10.80	-2.4	2.1	0.9	10.30	0.69	0.47	10.80	-2.9
oujhan	4.093	2014	185	10.95	13.09	**4.161**	5.7	4.19e+02	10.95	-2.2	2.2	1.0	10.45	0.36	0.01	10.95	-2.9
hannu2	3.627	2014	185	11.34	13.36	**3.670**	6.0	1.06e+03	11.33	-1.8	2.3	1.0	10.83	0.17	0.00	11.33	-3.0
nu2tar	3.240	2014	185	10.87	12.83	**3.268**	10.6	8.82e+02	10.87	-2.3	2.1	1.0	10.37	0.52	0.20	10.87	-2.9
tarbrz	2.893	2014	185	10.87	12.79	**2.911**	13.2	1.50e+03	10.87	-2.3	2.1	1.0	10.37	0.52	0.20	10.87	-2.9
brzsuw	2.607	2014	185	10.81	12.60	**2.620**	15.2	2.71e+03	10.82	-2.4	2.1	0.9	10.32	0.66	0.43	10.82	-2.9
belzag	2.173	2014	185	11.39	12.92	**2.178**	21.2	6.63e+03	11.38	-1.7	2.3	1.0	10.88	0.15	0.00	11.38	-3.0
kilpel	5.691	2014	185	11.04	13.11	**5.844**	14.8	3.98e+00	11.03	-2.1	2.2	1.0	10.53	0.29	0.00	11.03	-2.9
muopel	5.450	2014	185	11.05	13.17	**5.596**	14.8	5.64e+00	11.05	-2.1	2.2	1.0	10.55	0.28	0.00	11.05	-2.9
oujhan	4.093	2014	185	11.20	13.34	**4.161**	4.9	5.68e+02	11.20	-1.9	2.3	1.0	10.70	0.21	0.00	11.20	-3.0
hannu2	3.627	2014	185	11.51	13.53	**3.667**	6.0	1.06e+03	11.50	-1.5	2.4	1.0	11.02	0.11	0.00	11.52	-1.2
nu2tar	3.240	2014	185	11.12	13.08	**3.267**	9.1	1.20e+03	11.12	-2.0	2.2	1.0	10.62	0.24	0.00	11.12	-2.9
tarbrz	2.893	2014	185	11.12	13.04	**2.910**	12.4	1.70e+03	11.12	-2.0	2.2	1.0	10.62	0.24	0.00	11.12	-2.9
brzsuw	2.607	2014	185	11.08	12.87	**2.619**	15.2	2.72e+03	11.08	-2.0	2.2	1.0	10.58	0.26	0.00	11.08	-2.9
kilpel	5.691	2014	185	11.29	13.36	**5.844**	14.6	4.09e+00	11.28	-1.8	2.3	1.0	10.78	0.18	0.00	11.28	-3.0
muopel	5.450	2014	185	11.15	13.27	**5.595**	14.6	5.80e+00	11.15	-2.0	2.2	1.0	10.65	0.23	0.00	11.15	-2.9
oujhan	4.093	2014	185	11.45	13.59	**4.160**	4.8	5.93e+02	11.45	-1.6	2.3	1.0	10.95	0.13	0.00	11.45	-3.0
nu2tar	3.240	2014	185	11.21	13.17	**3.267**	9.1	1.20e+03	11.22	-1.9	2.3	1.0	10.72	0.21	0.00	11.22	-3.0
tarbrz	2.893	2014	185	11.37	13.29	**2.910**	11.7	1.91e+03	11.37	-1.7	2.3	1.0	10.87	0.16	0.00	11.37	-3.0
belzag	2.173	2014	185	11.45	12.98	**2.178**	21.2	6.63e+03	11.45	-1.6	2.3	1.0	10.95	0.13	0.00	11.45	-3.0

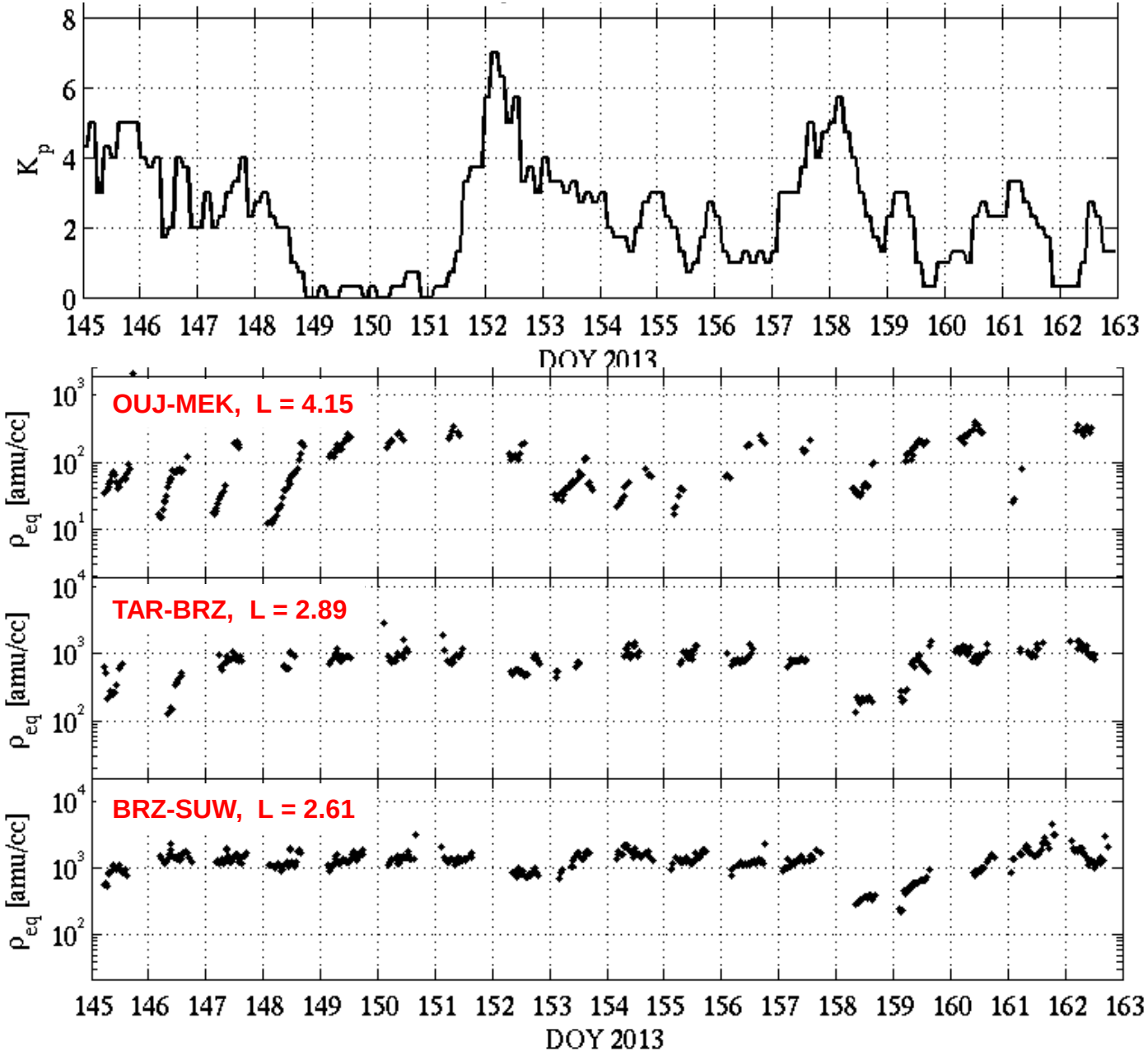
K_p
8
6
4
2
0
145 146 147 148 149 150 151 152 153 154 155 156 157 158 159 160 161 162 163
DOY 2013
OUJ-MEK, L = 4.15
TAR-BRZ, L = 2.89
BRZ-SUW, L = 2.61
ρ_{eq} [amu/cc]
10^3
10^2
10^1
10^4
10^3
10^2
10^4
10^3
10^2
145 146 147 148 149 150 151 152 153 154 155 156 157 158 159 160 161 162 163
DOY 2013

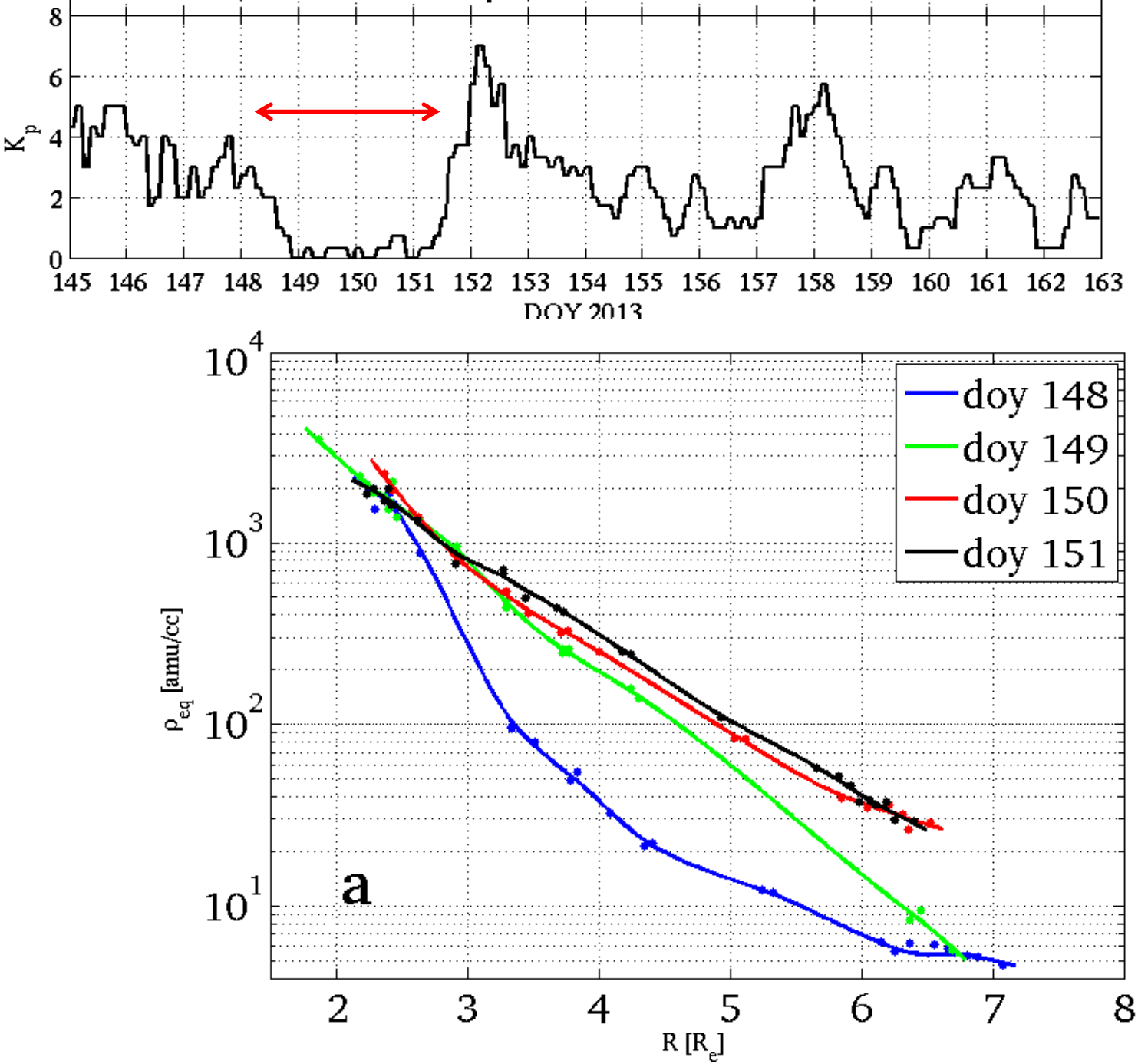
K_p
0
2
4
6
8
145 146 147 148 149 150 151 152 153 154 155 156 157 158 159 160 161 162 163
DOY 2013
ρ_eq [amu/cc]
10^4
10^3
10^2
10^1
doy 148
doy 149
doy 150
doy 151
a
2 3 4 5 6 7 8
R [R_e]

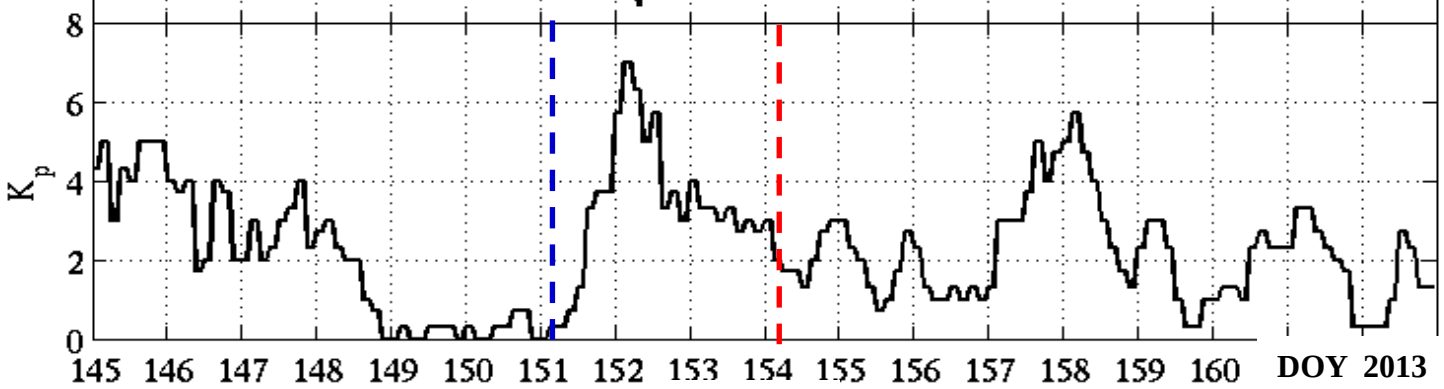
8
6
4
2
0
K_p
145 146 147 148 149 150 151 152 153 154 155 156 157 158 159 160
DOY 2013

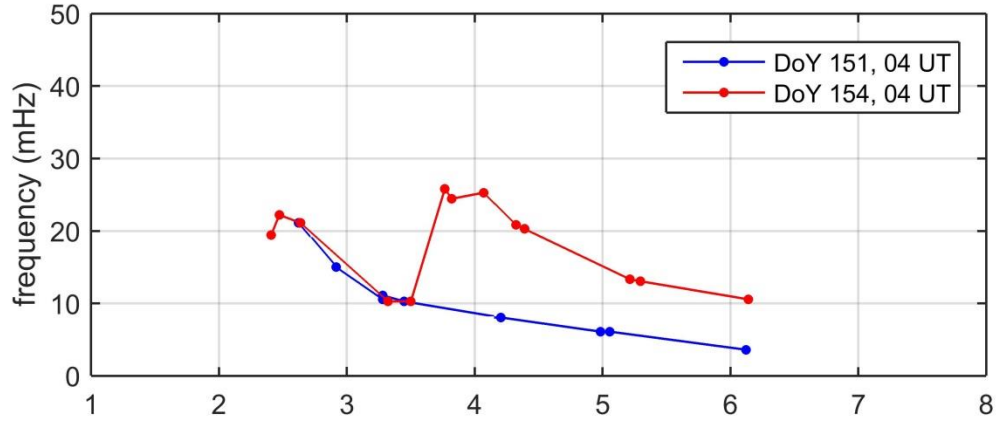
50
40
30
20
10
0
frequency (mHz)
1 2 3 4 5 6 7 8
DoY 151, 04 UT
DoY 154, 04 UT

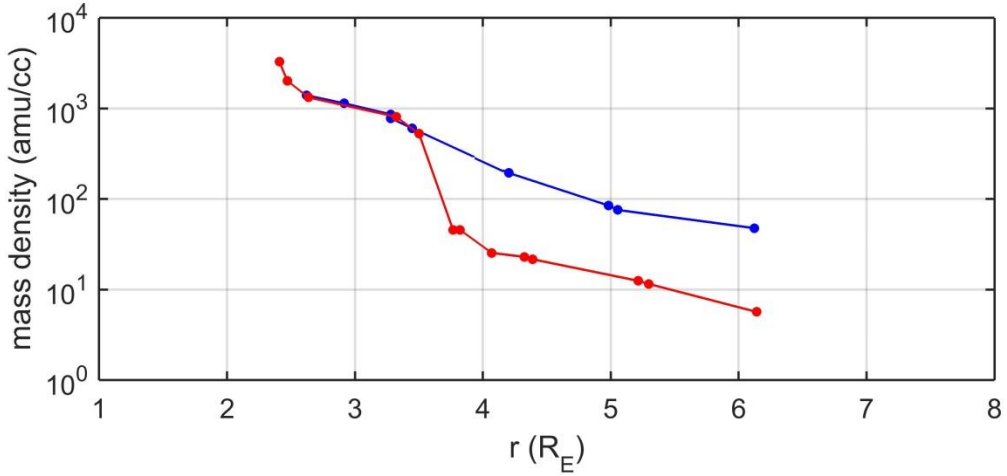
10^4
10^3
10^2
10^1
10^0
mass density (amu/cc)
1 2 3 4 5 6 7 8
r (R_E)

Comparison of FLR-derived plasma mass densities with in-situ electron densities

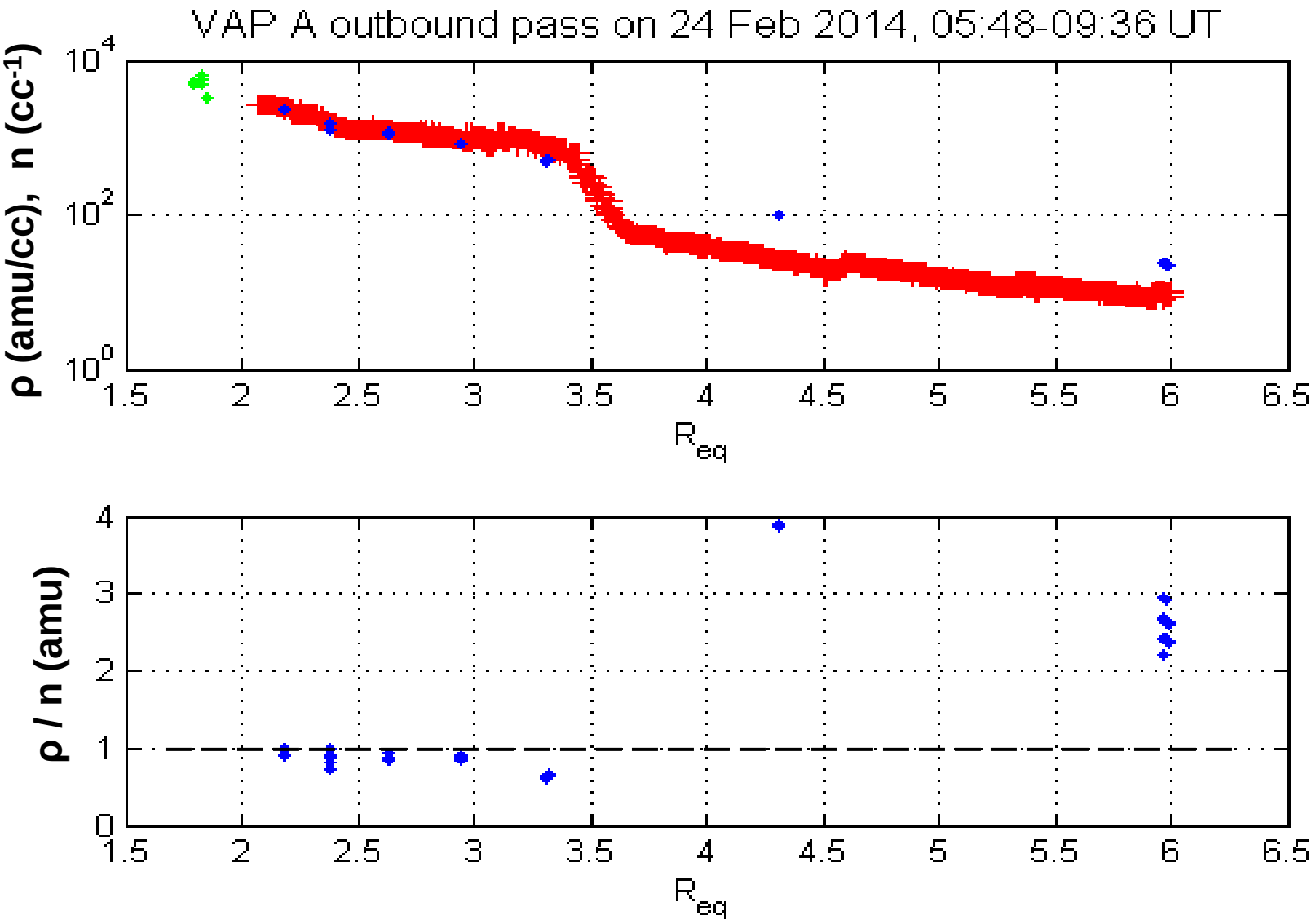

A comparison between

plasma mass densities (from EMMA-FLRs)

and electron densities (from VAP EMFISIS)

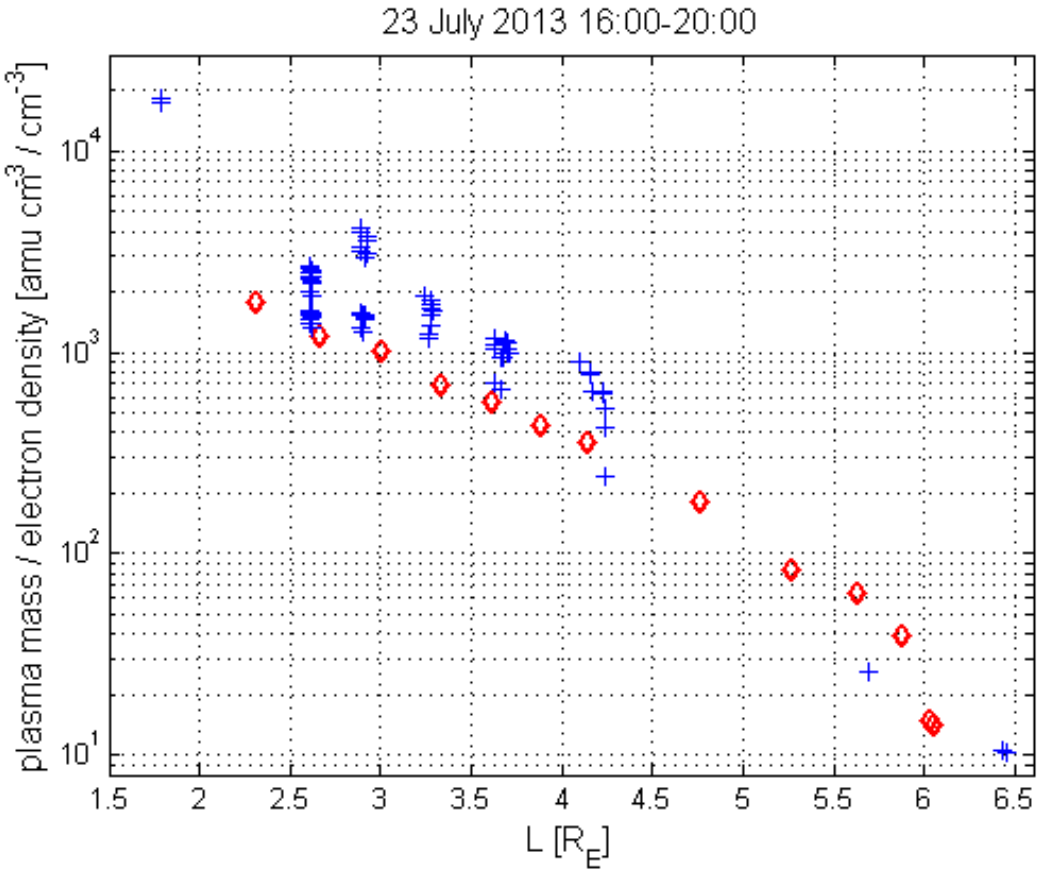

$$\frac{\rho_{eq}}{n_{eq}} = 1.5 - 2 \text{ amu}$$

Thank you for your attention